The American Journal of Human Genetics, Volume *108*

Supplemental information

Bi-allelic variants in the ER quality-control mannosidase gene *EDEM3* cause a congenital disorder of glycosylation

Daniel L. Polla, Andrew C. Edmondson, Sandrine Duvet, Michael E. March, Ana Berta Sousa, Anna Lehman, CAUSES Study, Dmitriy Niyazov, Fleur van Dijk, Serwet Demirdas, Marjon A. van Slegtenhorst, Anneke J.A. Kievit, Celine Schulz, Linlea Armstrong, Xin Bi, Daniel J. Rader, Kosuke Izumi, Elaine H. Zackai, Elisa de Franco, Paula Jorge, Sophie C. Huffels, Marina Hommersom, Sian Ellard, Dirk J. Lefeber, Avni Santani, Nicholas J. Hand, Hans van Bokhoven, Miao He, and Arjan P.M. de Brouwer

Figure S1. N-glycan analysis of fibroblasts from a control and an EDEM3 deficient individual.

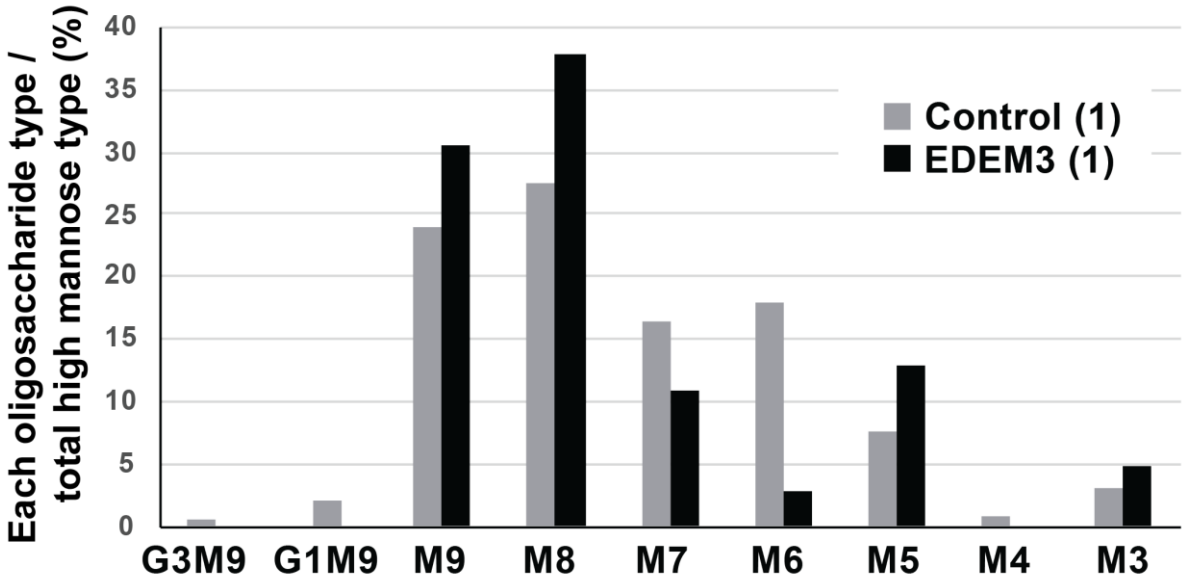

Mass spectrometry analysis of total N-glycans in fibroblasts from individual IV-2 of family 1 and a single control show accumulation of M9 and M8, and relatively lower M7 and M6 consistent with deficiency of EDEM3.

Figure S2. The representative N-glycan profiles of plasma from normal and EDEM3-CDG affected individuals.

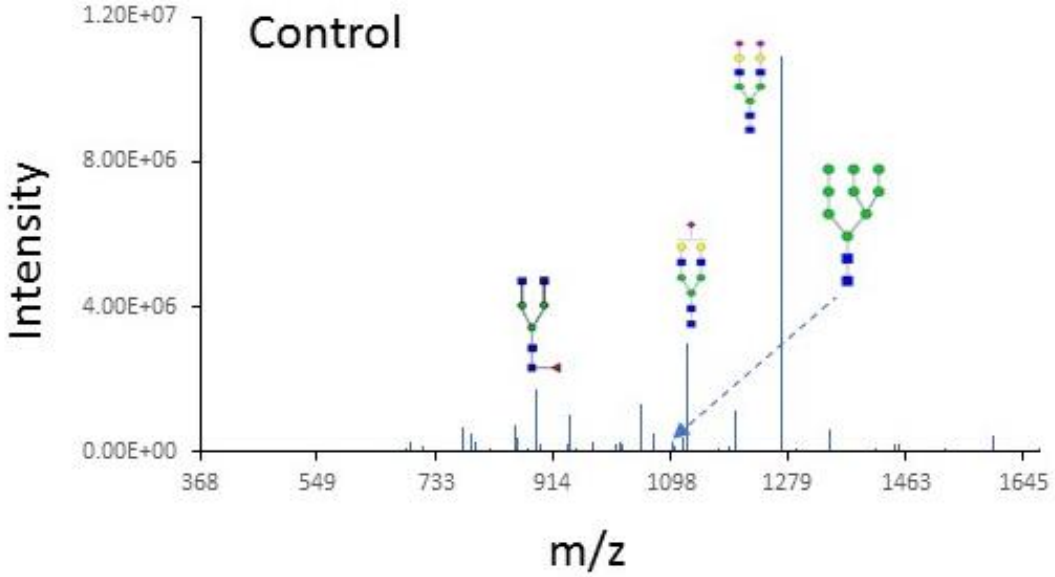

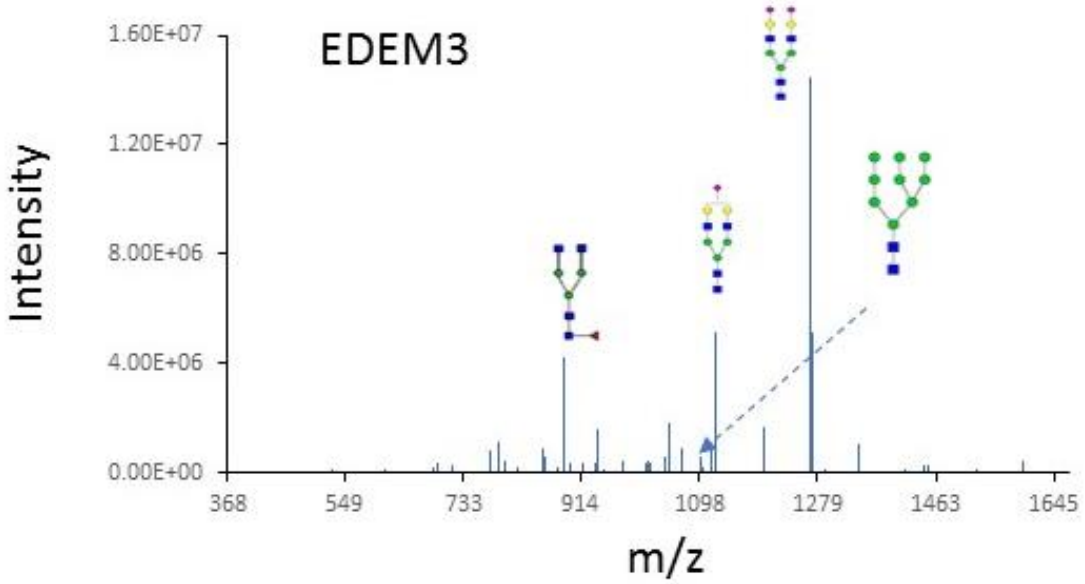

.
The overall abundance of complex glycans is normal in plasma EDEM3-CDG affected individuals.

Figure S3a. Characterization of the G1M5 structure in EDEM3 deficient cell lines.

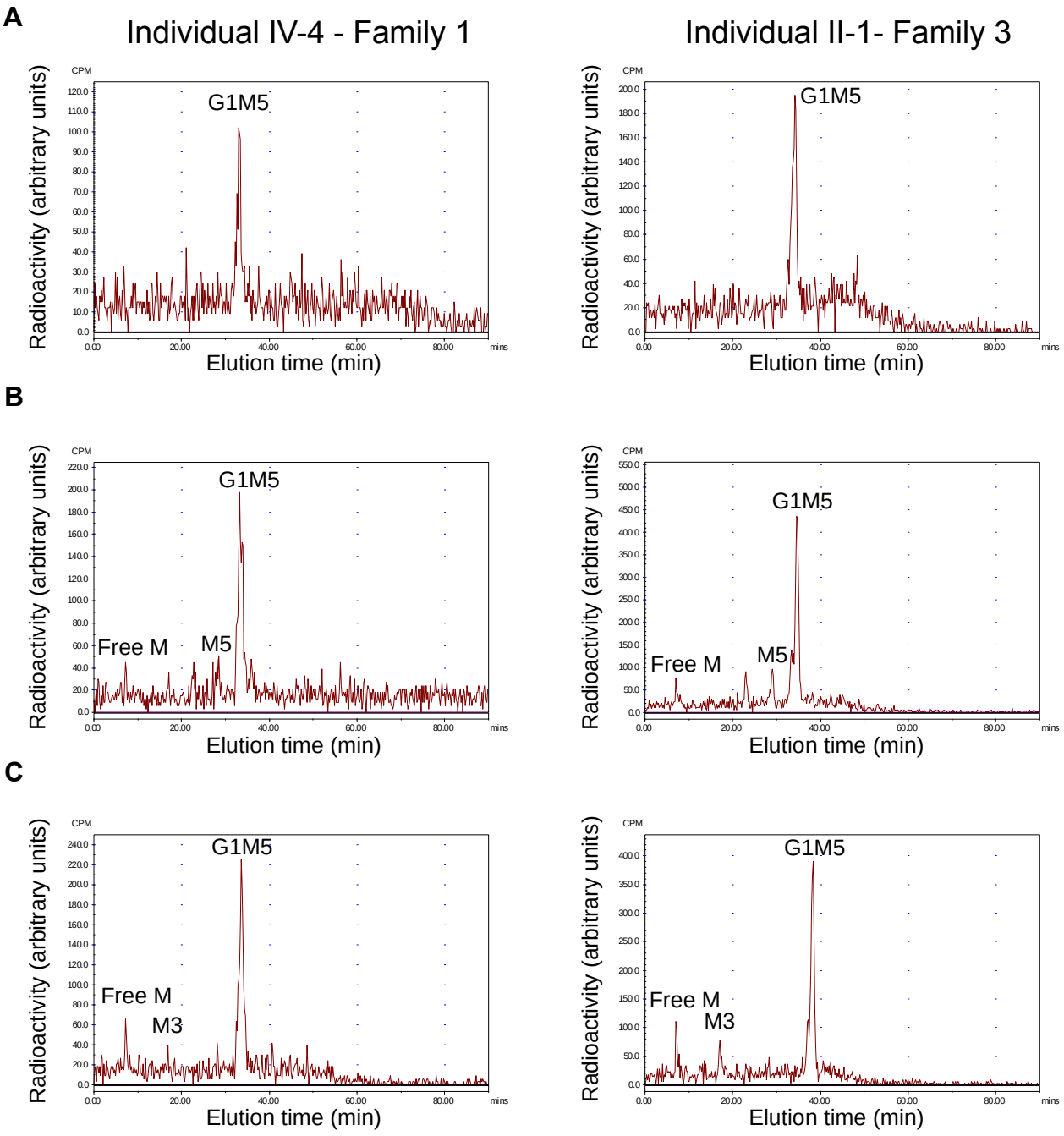

Patient fibroblasts from family 1 (individual IV-4) and family 3 (individual II-1) were incubated with [2-^{3}H] mannose for 1h and chased during 2h. A) HPLC profile of the G1M5 peak obtained from N-glycoproteins collected and isolated by HPLC analysis. B) HPLC profile of the isolated G1M5 after treatment with saitoi α1,2-mannosidase. C) HPLC profile of the isolated G1M5 peak after treatment with jack bean α-mannosidase. The G1M4 peak is not visible as jack bean α-mannosidase has difficulties in cleaving the α1,6-mannose residue after 2h. The M3, M5, and free M peaks are derived from M6, which is isolated together with the G1M5 peak.

Figure S3b. **Characterization of the M5 structure in EDEM3 deficient cell lines**.

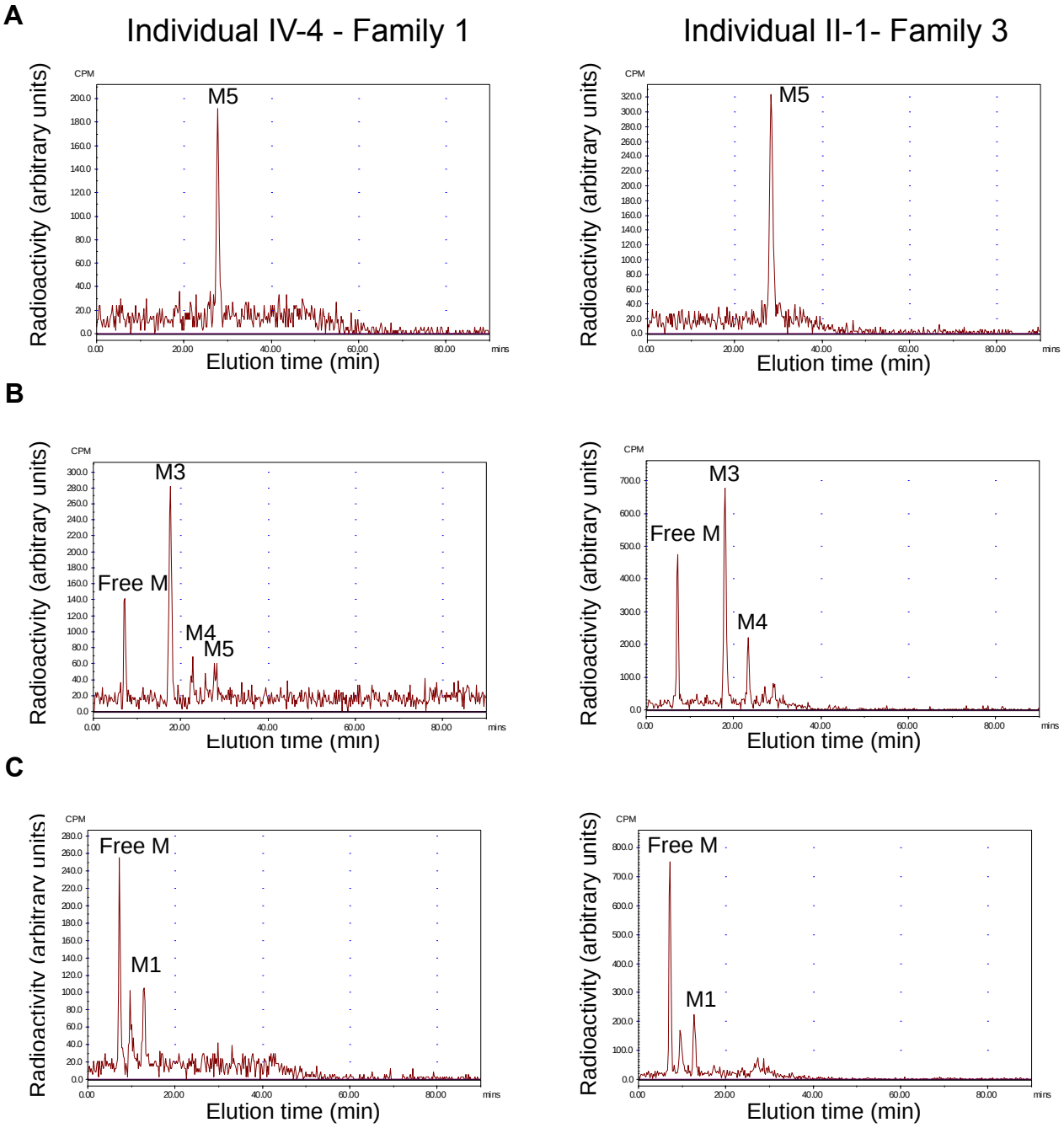

Patient fibroblasts from family 1 (individual IV-4) and family 3 (individual II-1) were incubated with [2-^{3}H] mannose for 1h and chased during 2h. A) HPLC profile of the M5 peak obtained from N-glycoproteins collected and isolated by HPLC analysis. B) HPLC profile of the isolated M5 after treatment with saitoi α1,2-mannosidase. C) HPLC profile of the isolated M5 peak after treatment with jack bean α-mannosidase

Figure S4. Deletion of 47bp in mouse *Edem3* exon 3 results in a protein null.

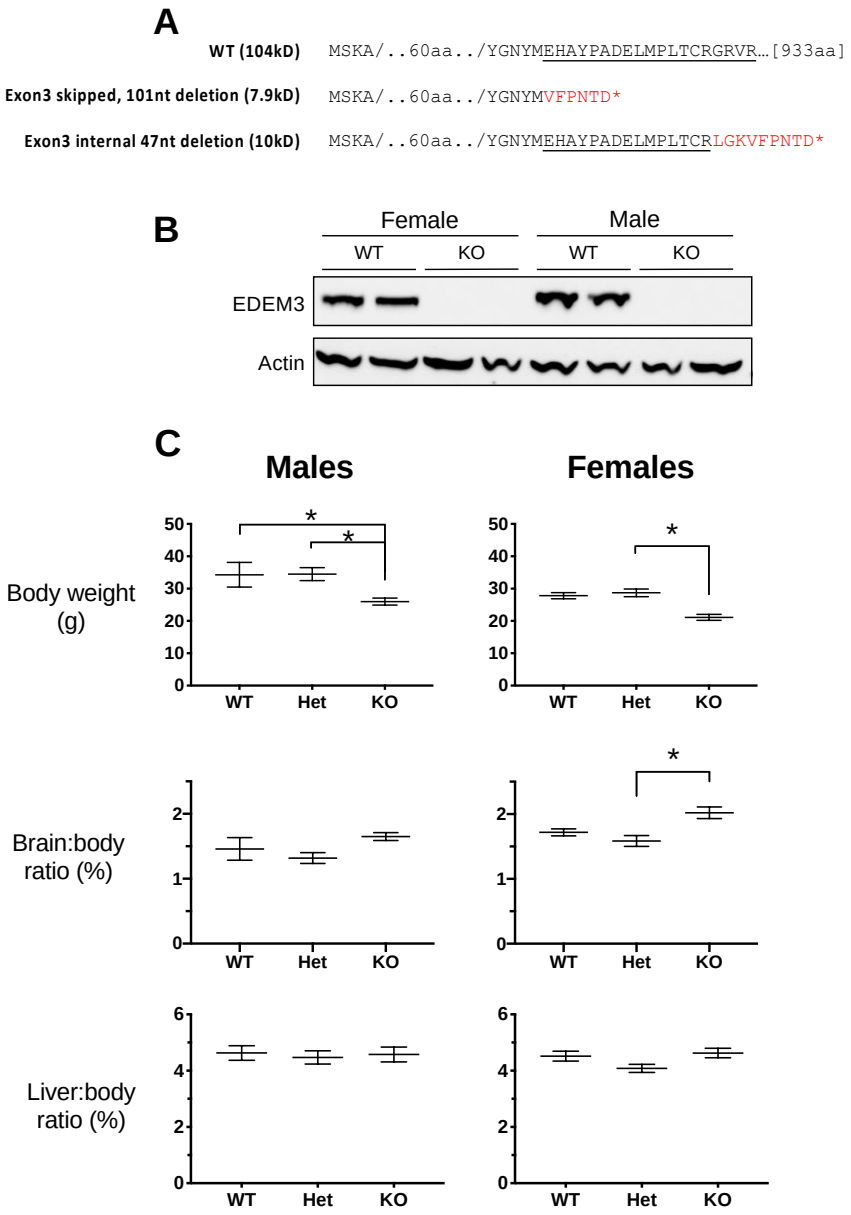

A) Predicted polypeptide sequences from splice variants detected in liver from homozygous *Edem3* KO mice, either with *Edem3* exon 3 skipped, or the exon 3 with in a internal 47bp deletion (*Edem3* KO allele), relative to the reference transcript (WT). Underlined text=exon 3 (partial sequence); red text=frameshifted sequence. B) Western blot using a polyclonal rabbit antibody against EDEM3 of 100µg of protein from control or *Edem3* KO mouse liver lysate. Two wildtype females and two wildtype males are compared with two knock-out females and two knock-out males showing that there is no expression of Edem3 protein in the liver of knock-out animals. C) Body weight, brain weight adjusted to body weight (expressed as a percentage), and liver weight adjusted to body weight (expressed as a percentage) of male and female mice is given. Wild-type (WT), heterozygous (Het), or knockout (KO) for *Edem3* aged between 52 and 80 weeks at time of sac are shown. The age of the mice did not differ significantly between genotypes in either sex. The body weight of the KO mice was significantly lower than that of heterzygous mice in both sexes, and that of WT male mice, suggesting a mild kachexia phenotype. Brain to body weight in female KO was modestly but significantly increased. One-way ANOVA, Tukey's multiple comparison test, *P<0.05. Male mice: WT n=5; Heterozygous n=4; KO n=6. Female mice: WT n=6; Het n=13; KO n=4.

Figure S5. N-glycan analysis of *Edem3* KO and WT mice.

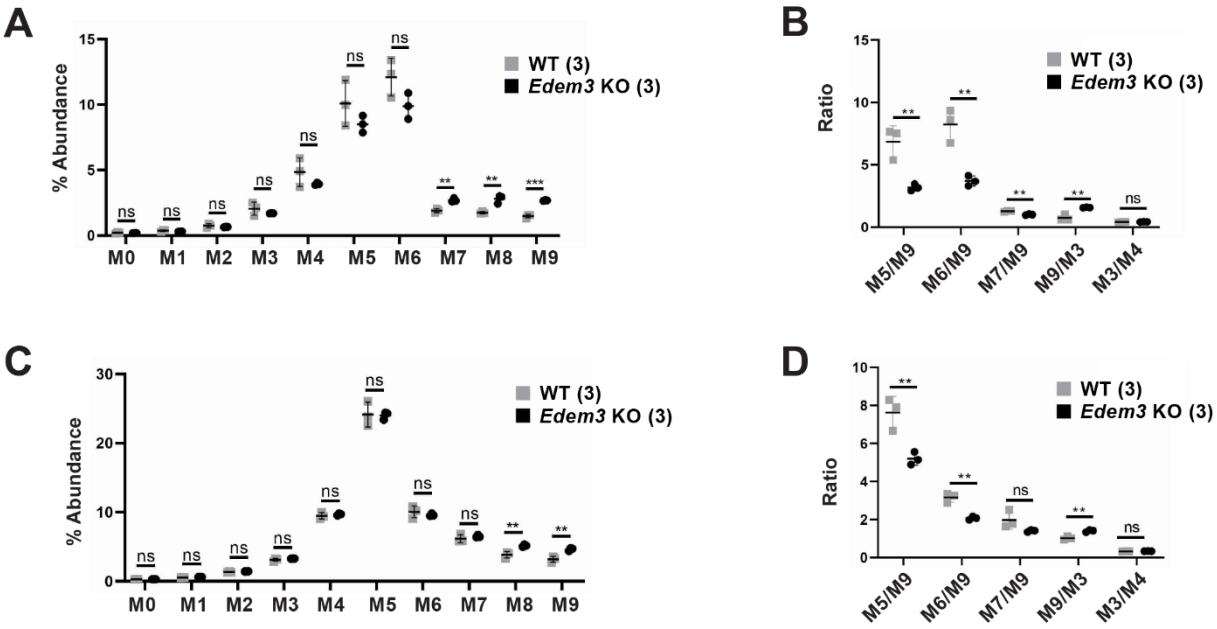

A) Abundance of murine plasma n-glycan species. B) Ratio of murine plasma n-glycan species. C) Abundance of murine brain n-glycan species. D) Ratio of murine brain n-glycan species. Bars indicate mean values. Error bars represent standard deviation. Indicated P-values from Student's T-test, ns = not significant; **P*<0.05; ***P*<0.01; ****P*<0.001.

Supplemental material and methods

Exome Sequencing (ES), Filtering, and Annotation

High-throughput sequencing was performed for sibling pairs of families 1 and 2 at BGI (BGI-Shenzhen, Shenzhen, China). Exome capturing was carried out by using Agilent SureSelect Target Enrichment V5 (Agilent Technologies, Santa Clara, CA, USA). Sequencing was performed by using the Illumina HiSeq 2000 platform (Illumina, San Diego, CA, USA). Illumina base calling software v1.7 was employed to analyze the raw image files with default parameters. Data analysis was performed using the Roche Newbler software (v.2.3) using human genome build hg19/GRCh37. Selection of the variants was performed by using a seven tier filtering strategy as previously described [1]. Potential causative variants found by ES were confirmed by Sanger sequencing. Primers were designed by using the online software Primer3plus [2]. Amplifications were performed using standard methods. PCR products were visualized by gel electrophoresis. Subsequently, enzymatic DNA purification with ExoI (New England BioLabs, Ipswich, MA, USA) and Fast AP (ThermoFischer Scientific, Waltham, MA, USA) was carried out using a thermal cycler starting with incubation at 37 °C for 15 minutes followed by an additional 15 minutes incubation at 80 °C. PCR products were sequenced using the ABI PRISM BigDye Terminator Cycle Sequencing V2.0 Ready Reaction Kit and analyzed with the ABI PRISM 3730 DNA analyzer (Applied Biosystems, Foster City, CA, USA).

ES for family 3 was performed as a trio with patient 6 and his parents at the Children's Hospital of Philadelphia. Exome capture was performed using the Agilent SureSelect XT Clinical Research Exome kit per manufacturer's protocol (Agilent Technologies, Santa Clara, CA, USA) and sequenced on the Illumina HiSeq 2000 or 2500 platform with 100bp paired-end reads (Illumina, San Diego, CA, USA). Mapping and analysis were based on the human genome build UCSC hg19 reference sequence. Potential causative variants found by ES were confirmed by Sanger sequencing as was the presence of the *EDEM3* variants in affected siblings, patients 7 and 8. Read alignment and variant calling were performed with an in-house bioinformatics pipeline incorporating NovoAlign (Novocraft, Selangor, Malaysia,

http://www.novocraft.com/) for read alignment; Picard (Broad Institute, Cambridge, MA) for marking duplicates; and Genome Analysis Toolkit's (GATK) (Broad Institute, Cambridge, MA) [3,4]. Best Practices for UnifiedGenotyper, with no parameter modifications, for variant calling (reference sequence: hg19/GRCh37) and variant filtering based on read depth (≥5X). Variant filtration was performed with an in-house bioinformatics pipeline. Analysis was performed as previously described [5].

Family 4 underwent trio exome sequencing at Ambry Genetics (Aliso Viejo, CA, US) as part of a research contract in a study protocol (H15-00092) approved by the University of British Columbia. Coding regions were captured with IDT xGen Exome Research Panel v1.0 (Coralville, IA, US). Sequencing on an Illumina (San Diego, CA, USA) platform was performed to the depth such that 99% of consensus coding regions were sequenced at least 10X. Alignment of 150bp reads to the reference genome (GRCh37/Hg19) and variant calling was performed with BWA-MEM (35), GATK, SAMtools, and Picard, and then annotated and prioritized with VarSeq v.1.5 (Golden Helix, Bozeman, MT, US) [3].

For family 5, the patient's genomic DNA was analyzed in comparison with the published human genome build GRCh37/hg19. Using a custom-developed analysis tool (XomeAnalyzer; GeneDx, Gaithersburg, MD, USA), data were filtered and analyzed to identify sequence variants and most deletions and duplications involving three or more coding exons [6]. Reported clinically significant variants were confirmed by an appropriate orthogonal method in the proband and in selected relatives as necessary. Sequence and copy number variants are reported according to the Human Genome Variation Society (HGVS) or International System for Human Cytogenetic Nomenclature (ISCN) guidelines, respectively.

Trio exome sequencing was performed for family 6 using the Twist Human Core Exome Kit (Twist Bioscience, San Francisco, CA, USA). Sequencing of paired-end 150bp reads was performed on a NextSeq500 (Illumina, SanDiego, CA, USA). BWA-MEM (v0.7.12) [7] was used to de-multiplex and align Illumina NextSeq FASTQ reads to the reference genome (GRCh37/Hg19). After conversion to BAM file format and duplicate removal (Picard v1.129; http://broadinstitute.github.io/picard/), indel realignment, variant calling and quality filtering was

performed using GATK (v3.4-46) [3]. Variant annotation was performed using Alamut Batch (Interactive Biosoftware, Rouen, France) and variant filtering was performed as previously described [8,9].

Duo exome capturing was carried out for family 7 by using Agilent SureSelect Target Enrichment Clinical Research Exome V2 (Agilent Technologies, Santa Clara, CA, USA). Sequencing (paired-end 150bp) was performed by the Illumina HiSeq 4000 platform (Illumina, San Diego, CA, USA). Data was demultiplexed by Illumina Software CASAVA. Reads are mapped to the genome (hg19/GRCh37) with the program BWA (http://bio-bwa.sourceforge.net/). Variants are detected with the Genome Analysis Toolkit (http://www.broadinstitute.org/gatk/). Subsequently, variants were filtered with the Alissa Interpret software package (Agilent Technologies, Santa Clara, CA, USA) and were further selected based on two inheritance models (autosomal recessive and X-linked recessive/dominant).

Cell lines and culture maintenance

Epstein-Barr-virus-transformed lymphoblastoid (EBV-LCL) cell lines derived from patients and fibroblast cell lines were grown in Dulbecco's Modified Eagle Medium (DMEM) supplemented with 10% (volume/volume) fetal calf serum (catalog no. F7524; Sigma Aldrich, St. Louis, MO, USA), 1% (volume/volume) sodium pyruvate (catalog no. S8636; Sigma Aldrich, St. Louis, MO, USA), and penicillin/streptomycin (catalog no. P4333; Sigma Aldrich, St. Louis, MO, USA). To analyze the effect of nonsense-mediated mRNA decay (NMD) on the gene expression, 1 µg/ml cycloheximide (C4859-1 ml; Sigma Aldrich, St. Louis, MO, USA), an inhibitor of NMD, is used to inhibit degradation of nonsense RNA in five fibroblasts lines for 4 hours. To analyze the potential effect on the cellular stress response mechanism, 4 µg/ml tunicamycin (catalog no. T7765-5MG; Sigma Aldrich, St. Louis, MO, USA) was used to induce stress in three control and three EBV-LCL lines, and six controls and six fibroblasts lines for 5 hours after which the cells were harvested [10,11].

RNA isolation, cDNA Synthesis and quantitative real time PCR (qPCR)

All RNA isolations were performed with the NucleoSpin RNA Clean-up Kit (catalog no. 740955-50, Macherey-Nagel, Düren, Germany) according to manufacturer's protocol. RNA was quantified by NanoDrop (Thermo Fisher Scientific, Waltham, MA, USA). Considering that the mutations are predicted to trigger NMD, we examined the expression level of *EDEM3* mRNA using qPCR analysis. Total RNA was isolated from EBV-LCL from the proband and two affected siblings of family 1, and fibroblast cell lines of individual IV-4 from family 1 and of individuals II-1 and II-2 from family 3 with or without cycloheximide (CHX). For qPCR, 2 µg total RNA was reverse transcribed into cDNA using the SuperScript VILO Master Mix (catalog no. 11755050, Thermo Fisher Scientific, Waltham, MA, USA), following manufacturer's instructions. Amplifications were performed in duplicates of 25 µl reactions in the presence of SYBR green (Applied Biosystems, Foster City, CA, USA), using the absolute quantification setting on an ABI PRISM 7900HT Sequence Detection System (Applied Biosystems, Foster City, CA, USA), using the ΔΔCt method, as described before [12], to quantify differences in gene expression compared to housekeeping genes *GUSB*, *PPIB* and *CLK2*. Additionally, to test the potential effect of the *EDEM3* mutations in the UPR stress response of the cells [10,11], qPCR analysis was performed using primers located in the *IRE1*, *ATF6* and *PERK* genes, in cDNA collected from EBV-LCL cells derived from three affected family members and three healthy EBV-LCL controls; all treated with and without tunicamycin. Results were analyzed using the ΔΔCt method described previously[12,13]. Primer sequences are available upon request.

Antibodies and Western blot analysis

Anti-EDEM3 antibodies were purchased from Signalway Antibody LLC (Maryland, USA), anti-β-actin antibodies from MilliporeSigma (Burlington, MA, USA), and goat anti-rabbit or goat anti-mouse immunoglobins conjugated to h*orseradish peroxidase* (HRP) were ordered from Agilent Technologies (Santa Clara, CA, USA). Cells were pelleted and lysed in RIPA Buffer (50 mM Tris-HCl pH 7.9, 120 mM NaCl, 1% NP40, 1 mM EDTA, 1 mM Na_3VO_4, 55 mM NaF) supplemented with a cocktail of protease inhibitors (Roche, Meylan, France). Cells were

centrifuged at 20,000g and 4°C for 10 min. The protein concentration contained in the supernatant was determined with a MicroBCA™ Protein Assay Reagent kit (Thermo Fisher Scientific, Waltham, MA USA). Twenty micrograms of total protein of each sample were dissolved in reducing NuPage Sample buffer and separated on 4-12% Bis-Tris gel (Thermo Fisher Scientific, Waltham, MA, USA) and transferred to nitrocellulose membranes Hybond ECL (GE Healthcare, Little Chalfont, UK). Membranes were blocked using Tris-buffered saline (TBS) containing 0.05% Tween20 and 5% (w/v) bovine serum albumin (BSA). Primary antibodies rabbit anti-EDEM3 and mouse anti-actin (for quantification) were incubated overnight at 4°C in TBS, 0.05% Tween20 (TBS-T) and 5% (w/v) BSA at respectively 1:500 and 1:10,000 dilution. Menbranes were washes three times 5 min in TBS-T after addition of the primary and secondary antibodies. Either goat anti-rabbit IgG and goat anti-mouse IgG HRP conjugated were used as secondary antibodies at dilution of 1:5,000 and 1:20,000. Signal was detected by a chemilescence reagent (PierceTM Pico Plus Westernblotting Substrate ; Thermo Fisher Scientific, Waltham, MA, USA) on a imagin film (GEHealthcare, Buckinghamshire, UK).

Alpha-mannosidase treatment of N-glycans

N-glycans were incubated in 200 µL 50 mM ammonium acetate buffer pH 4.5 with 0.5 U of jack bean α-mannosidase (EC 3.2.1.24, Sigma Aldrich, St. Louis, MO, USA) or in 200 µL of 20 mM sodium acetate buffer pH 5 with 0.5 U of α1,2-mannosidase (EC 3.2.1.113, isolated from Aspergillus saitoi, Glyko, UK). Enzyme digestions were carried out at 37 °C for 24 h with a fresh aliquot of enzyme added after 16 h. Released glycans were then analysed by HPLC.

Development of a novel mouse model of Edem3 genetic deficiency

A mouse model of *Edem3* genetic deficiency was generated at the Transgenic and Chimeric Mouse Facility of the University of Pennsylvania, by coinjection into fertilized C57BL6/J zygotes of spCas9 mRNA (TriLink Biotechnologies, San Diego, CA), along with RNA oligos corresponding to tracrRNA and two separate *Edem3* guide RNAs (GR5, 5'-GCCUCUGACACGGCCCCGGC and GR6, 5'-GGGCGAUGUGGAUGACGCCU; Integrated

DNA Technologies, Coralville, IA). Founder mice with biallelic deletion of a 47bp DNA sequence between the GR5 and GR6 gRNA target sequences, were identified by PCR of genomic DNA, and confirmed by Sanger sequencing. The deleted sequence (GGGGCCGTGTCAGAGGCCAGGAGCCCAGCCGGGGCGATGTGGATGAC) results in a frameshift deletion within *Edem3* exon 3 (which is present in all predicted *Edem3* transcripts). Liver RNA was reverse transcribed, and a region of *Edem3* cDNA was amplified with transcript-specific primers (mmEDEM3F376, 5'-TGATCATGCTT-ATGGCAACTATATG and mmEDEM3R822 5'-AACTTTAAATTAATCCTGGGGTACG). PCR products were cloned by TopoTA cloning, and Sanger sequencing demonstrated the presence of two transcript variants, the first of these confirmed transcription of the deleted DNA, while the second revealed a novel splice variant in which the partially deleted exon 3 was skipped, with direct splicing of exon 2 to exon 4 (leading to a 101 nucleotide deletion relative to the reference transcript). Importantly, both of these splice variants lead to early frameshifts, Arg84fs*9 in the case of the 47nt deletion, and Met69fs*5 for the exon2-exon4 splice variant. The biallelic 47bp deletion was confirmed to result in a protein null by Western blot of liver lysate with a rabbit polyclonal directed against a conserved C-terminal region (amino acids 854-903 of Human EDEM3 protein according to Q9BZQ6; ab118762, Abcam, Boston, MA). These data are summarized in **Supplemental Figure S3.**

While the biallelic 47bp deletion was compatible with life, and the escaping *Edem3* knockout (KO) mice had no overt phenotypes, we note that *Edem3* KO pups were consistently recovered at considerably lower than the expected Mendelian ratio, suggesting that there is a strong development selection for EDEM3 function. *Edem3* KO females crossed to an *Edem3* heterozygous male produced 4.8% KO pups (expected 50%, P <0.0001), the reciprocal cross (KO male crossed to heterozygous females) yielded KO pups at 8.8% (expected 50%, P <0.0001), and heterozygous male to heterozygous females generated 1.7% KO pups (expected 25%, P =0.0002).

Culturing of fibroblasts

All fibroblasts were cultured in high glucose DMEM (D0819, Sigma-Aldrich) supplemented with 20% fetal calf serum (FCS; F7524, Sigma-Aldrich), 1% penicillin/streptomycin (P/S; P4333, Sigma-Aldrich) and 1% sodium pyruvate (S8636, Sigma-Aldrich). Fibroblasts were incubated at 37°C/5% CO_2. After transduction fibroblasts were cultured in the same conditions, with medium supplemented with 0.5 µg/ml puromycin (P9620; Sigma-Aldrich).

Transduction of patient fibroblasts with hEDEM3

Lentiviral constructs with hEDEM3 (NM_001319960.2) driven by a human cytomegalovirus (CMV) promoter and with a puromycin resistance gene were constructed and generated by VectorBuilder (>10^8 TU/ml in Hanks' Balanced Salt solution; HBSS buffer). An enhanced green fluorescent (eGFP) control lentivirus (VB160109-10005, VectorBuilder) was used to control for transduction efficiency. Patient fibroblasts were seeded at a density of 10^5 cell per well of a 6-well plate (353046, Corning) the day before transduction. Transduction was done overnight in medium supplemented with 5 µg/ml polybrene (VectorBuilder). Two days after transduction, selection of transduced cells was started with increasing concentrations of puromycin (0.5 µg/ml – 2 µg/ml).

N-glycan profiling of cultured skin fibroblasts

Fibroblasts of a healthy control and of EDEM3-CDG individual IV-2 of family 1 (about 10 million of cells) were harvested by scraping. Protein denaturation and N-glycan release were performed according to Abu Bakar *et al* [14]. Released N-glycans were purified and enriched using graphitized carbon cartridges and N-glycans were eluted using 40% acetonitrile and 0.05% trifluoroacetic acid. Mass spectrometry analysis of total fibroblast N-glycans was performed using a porous graphitized carbon (PGC) chip on an Agilent 1260 Infinity HPLC-chip on an Agilent 6540 QTOF mass spectrometer (Agilent Technologies, Santa Clara, CA,

USA). MS data were analyzed using Agilent Mass Hunter Qualitative Analysis Software. Relative glycan abundances were calculated as described before [15].

Pulse-chase labeling analysis of N-glycans in cultured human fibroblasts

Fibroblast cell lines were preincubated at 0.5 mM glucose for 45 min and then metabolically labeled for 1h with 3.7 MBq/mL (2.25 μM) [2-3H] mannose at the same glucose concentration. When a chase was performed, pulse-labeled cells were washed twice with phosphate-buffered saline pH 7.4 (PBS) and incubated for 2h in DMEM medium containing 5 mM glucose. Sequential extraction and purification of oligosaccharide material were performed as described previously [16]. The protein pellet was digested overnight at room temperature with trypsin (1 mg/mL) in 0.1 M of ammonium bicarbonate buffer, pH 7.9. Subsequently, glycopeptides were treated overnight at 37°C with 0.5 U PNGase F in a 50 mM phosphate buffer, pH 7.2, to release oligosaccharides. The oligosaccharide fractions were then desalted on Bio-Gel P2 with 5% acetic acid. The analysis of the oligosaccharides was performed by high-performance liquid chromatography (HPLC) on an amino-derivatized Asahipak NH2P-50 column (250 mm×4.6 mm; Asahi, Kawasaki-Ku, Japan) with an acetonitrile/water gradient from 70:30 (v/v) to 50:50 (v/v) at a flow rate of 1 mL/min over 90 min. Elution of the radiolabeled oligosaccharides was monitored by continuous-flow detection of the radioactivity with a flo-one detector (Perkin-Elmer, Les Ullis, France).

Semi-quantitative analysis of N-glycans in human and mouse plasma and mouse brain tissue

N-glycans were prepared from heparinized plasma and analyzed as previously described **[17]**. Briefly, plasma samples were combined with internal standard of [^{13}C]-sialylglycopeptide, digested with Rapid PNGase FTM, reacted with RapiFluor-MS reagent, and subsequently flow injected and analyzed with a Waters Synapt G2 Si electrospray-ionisation quadrupole time-of-flight mass spectrometry (ESi-QTOF) in positive ion mode. For N-glycan analysis on mouse brain, whole brain was lysed in water by sonication and lysate of 200 μg of protein was subject to PNGaseF digestion and N-glycan analysis as described above.

Statistical testing

After log transformation, differences in gene expression by qPCR were tested with a student's t-test in excel. Student's t-test to measure the difference between the means in two independent samples was also used to analyze N-glycan performing pairwise comparisons of each glycan. Level of significance was uncorrected for multiple testing and set at $P \leq 0.05$.

References

1. Riazuddin, S., Hussain, M., Razzaq, A., Iqbal, Z., Shahzad, M., Polla, D.L., Song, Y., van Beusekom, E., Khan, A.A., and Tomas-Roca, L. (2016). Exome sequencing of Pakistani consanguineous families identifies 30 novel candidate genes for recessive intellectual disability. Mol. Psychiatry.

2. Untergasser, A., Cutcutache, I., Koressaar, T., Ye, J., Faircloth, B.C., Remm, M., and Rozen, S.G. (2012). Primer3--new capabilities and interfaces. Nucleic Acids Res *40*, e115.

3. Van der Auwera, G.A., Carneiro, M.O., Hartl, C., Poplin, R., Del Angel, G., Levy-Moonshine, A., Jordan, T., Shakir, K., Roazen, D., Thibault, J., et al. (2013). From FastQ data to high confidence variant calls: the Genome Analysis Toolkit best practices pipeline. Curr. Protoc. Bioinforma. *43*, 11.10.1-33.

4. McKenna, A., Hanna, M., Banks, E., Sivachenko, A., Cibulskis, K., Kernytsky, A., Garimella, K., Altshuler, D., Gabriel, S., Daly, M., et al. (2010). The Genome Analysis Toolkit: A MapReduce framework for analyzing next-generation DNA sequencing data. Genome Res. *20*, 1297–1303.

5. Gibson, K.M., Nesbitt, A., Cao, K., Yu, Z., Denenberg, E., DeChene, E., Guan, Q., Bhoj, E., Zhou, X., Zhang, B., et al. (2018). Novel findings with reassessment of exome data: implications for validation testing and interpretation of genomic data. Genet. Med. Off. J. Am. Coll. Med. Genet. *20*, 329–336.

6. Retterer, K., Scuffins, J., Schmidt, D., Lewis, R., Pineda-Alvarez, D., Stafford, A., Schmidt, L., Warren, S., Gibellini, F., Kondakova, A., et al. (2015). Assessing copy number from exome sequencing and exome array CGH based on CNV spectrum in a large clinical cohort. Genet. Med. Off. J. Am. Coll. Med. Genet. *17*, 623–629.

7. Li, H., and Durbin, R. (2009). Fast and accurate short read alignment with Burrows-Wheeler transform. Bioinforma. Oxf. Engl. *25*, 1754–1760.

8. Allen, H.L., Flanagan, S.E., Shaw-Smith, C., De Franco, E., Akerman, I., Caswell, R., International Pancreatic Agenesis Consortium, Ferrer, J., Hattersley, A.T., and Ellard, S. (2011). GATA6 haploinsufficiency causes pancreatic agenesis in humans. Nat. Genet. *44*, 20–22.

9. Stals, K.L., Wakeling, M., Baptista, J., Caswell, R., Parrish, A., Rankin, J., Tysoe, C., Jones, G., Gunning, A.C., Lango Allen, H., et al. (2018). Diagnosis of lethal or prenatal-onset autosomal recessive disorders by parental exome sequencing. Prenat. Diagn. *38*, 33–43.

10. Beriault, D.R., Dang, V.T., Zhong, L.H., Petlura, C.I., McAlpine, C.S., Shi, Y., and Werstuck, G.H. (2017). Glucosamine induces ER stress by disrupting lipid-linked oligosaccharide biosynthesis and N-linked protein glycosylation. Am. J. Physiol. Endocrinol. Metab. *312*, E48–E57.

11. Oslowski, C.M., and Urano, F. (2011). Measuring ER stress and the unfolded protein response using mammalian tissue culture system. Methods Enzymol. *490*, 71–92.

12. Livak, K.J., and Schmittgen, T.D. (2001). Analysis of relative gene expression data using real-time quantitative PCR and the 2(-Delta Delta C(T)) Method. Methods San Diego Calif *25*, 402–408.

13. Pfaffl, M.W. (2001). A new mathematical model for relative quantification in real-time RT-PCR. Nucleic Acids Res. *29*, e45.

14. Abu Bakar, N., Voermans, N.C., Marquardt, T., Thiel, C., Janssen, M.C.H., Hansikova, H., Crushell, E., Sykut-Cegielska, J., Bowling, F., MØrkrid, L., et al. (2018). Intact transferrin and total plasma glycoprofiling for diagnosis and therapy monitoring in phosphoglucomutase-I deficiency. Transl. Res. *199*, 62–76.

15. Ashikov, A., Abu Bakar, N., Wen, X.-Y., Niemeijer, M., Rodrigues Pinto Osorio, G., Brand-Arzamendi, K., Hasadsri, L., Hansikova, H., Raymond, K., Vicogne, D., et al. (2018). Integrating glycomics and genomics uncovers SLC10A7 as essential factor for bone mineralization by regulating post-Golgi protein transport and glycosylation. Hum. Mol. Genet. *27*, 3029–3045.

16. Kmiécik, D., Herman, V., Stroop, C.J., Michalski, J.C., Mir, A.M., Labiau, O., Verbert, A., and Cacan, R. (1995). Catabolism of glycan moieties of lipid intermediates leads to a single Man5GlcNAc oligosaccharide isomer: a study with permeabilized CHO cells. Glycobiology *5*, 483–494.

17. Chen, J., Li, X., Edmondson, A., Meyers, G.D., Izumi, K., Ackermann, A.M., Morava, E., Ficicioglu, C., Bennett, M.J., and He, M. (2019). Increased Clinical Sensitivity and Specificity of Plasma Protein N-Glycan Profiling for Diagnosing Congenital Disorders of Glycosylation by Use of Flow Injection-Electrospray Ionization-Quadrupole Time-of-Flight Mass Spectrometry. Clin. Chem. *65*, 653–663.